Supplemental Methods

Vectors and Cloning Retroviral shRNA libraries and individual shRNAs were cloned into MSCV-PM as previously described (Schlabach et al. 2008). The sublibrary shRNA library for the validation screen was synthesized (Agilent) followed by PCR-amplification of oligonucleotides released from microarrays using the forward primer siRNAF: CTAATTGATCTTCTCGAGAAGGTATATTGCTGTTGACAGTGAGCG and the reverse primer GFPr: TTTAAAGAATATACGCGTCCGCGTCGATCCTAGG. shRNAs were cloned into the XhoI/MluI sites of MSCV-PM-Mir30-PheS. The 3' mir30 sequence from MSCV-PM was added to this library using the FseI/EcoRI sites. Individual shRNAs from the validation screen for follow up experiments were synthesized as 100bp oligos (IDT) and cloned into the XhoI/EcoRI sites of MSCV-PM-PheS. All cloning was performed with enzymes from New England Biolabs, Qiaquick Gel Extraction kits from Qiagen, and DH5α bacteria from Invitrogen. pLXS-Neo HPV16 E6 and E7 were previously described (Smogorzewska and de Lange 2002). MSCV-mir30 based shRNA constructs as previously described (Paddison et al. 2004), MSCV-N terminal HA-FLAG-puro, pHAGE-C-terminal-HA-FLAG-Neo, pBABE-puro, pBABE USP28, and pBABE USP28^{C171A}. Retroviruses were packaged using 293T cells and Transit-293 (Mirus) transfection reagent according to the manufacturer's instructions.

Genomic DNA preparation Genomic DNA was harvested from initial and end samples by incubating in 10 mM Tris-HCl pH 8.0, 10 mM EDTA, 0.5% SDS, and 0.2 mg/ml proteinase K overnight at 55^{o}C, followed by the addition of 0.2 M NaCl. Genomic preps were phenol-chloroform extracted using Phase-Lock tubes (Fisher), treated with 25 μg/ml RNase A at 37^{o}C for 3 h, phenol-chloroform extracted again, ethanol precipitated, and resuspended in 10 mM Tris-HCl pH 8.5.

Half-hairpin barcode PCR, probe labeling, and microarray hybridization. Half-hairpin barcodes from the focused and genome scale screens were PCR-amplified from genomic DNA using the forward primer JH353F: TAGTGAAGCCACAGATGTA and the reverse primer BC1R: CCTCCCCTACCCGGTAGA, and 2 μg of the PCR product was Cy3- and Cy5-labeled

as previously described (Schlabach et al. 2008). Custom microarrays of half-hairpin probes were screened as previously described (Schlabach et al. 2008).

Multicolor Competition Assays for Nutlin-Resistance.
Multicolor competition assays (MCAs) were performed as described (Smogorzewska et al. 2007).

Growth Curves and SA-βgalactosidase assay Cell numbers were determined using a coulter counter and converted into PDs. Cells were fed every three days when not split. The SA-β-Gal assay was performed using the Senescent Cell Staining Kit (Sigma) according to the manufacturer's instructions. Experiments were carried out in triplicate and at least 100 cells were scored in each field, with error bars indicating s.e.m.

Immunoblotting and Antibodies Cell lysates were fractionated on 4-20% Tris-glycine SDS-PAGE gels (Invitrogen). Blocking (1 hour at room temperature), primary (overnight at 4°C) and secondary antibody (1 hour at room temperature) were all performed in TBST with 5 % milk. Antibodies were as follows: human p53 (DO-1 Calbiochem), human p21 (OP64 Calbiochem), human Mdm2 (Santa Cruz), human GATA4 (sc-9053, Santa Cruz), human p16 (sc-56330, Santa Cruz), human USP28 (A300-898A, Bethyl Laboratories), human Vinculin (Sigma-aldrich, V9131), human GAPDH (Santa Cruz, sc-25778), HRP-conjugated human and mouse secondary antibodies (Jackson), which were detected by chemilumiscence ECL reagent (Pierce).

References

Smogorzewska A, de Lange T. 2002. Different telomere damage signaling pathways in human and mouse cells. *EMBO J* **21**: 4338-4348.

Supplemental Figure 1. Genetic interrogation of replicative senescence in primary BJ fibroblasts.

(A) Western blot for the indicated proteins in BJ fibroblasts expressing either empty vector, or MSCV-HPV E6, or MSCV-HPV E7.

(B) Growth of mid-passage BJ fibroblasts expressing HPV E6 or **(C)** HPV E7 and shRNAs against luciferase (Luc), Rb, p53 or shRNA library pools as indicated.

Supplemental Figure 2.

(A) Growth of mid-passage BJ fibroblasts expressing HPV E7 and shRNAs against luciferase (FF), Rb, and p53 as indicated. **(B)** Plots of the log2 ratio enrichment scores for each shRNA in the focused set library screen in E7 BJ fibroblasts. **(C)** Plots of the log2 ratio enrichment scores for each shRNA in the focused set library screen in E6 BJ fibroblasts. **(D)** Known proliferation regulators that met our candidate criteria from the focused and genome library screens in E6 BJ fibroblasts. **(E)** Diagram showing cell cycle and DNA damage response components which were recovered from our focused and genome scale screens in E7 or E6 BJ fibroblasts. **(F)** Known p53 pathway and cell cycle genes that met our candidate criteria from the focused and genome library screens in E7 BJ fibroblasts. **(G)** Schematic showing the design of the multicolor competition assay. **(H)** Representative validation data from nutlin-resistance screens as shown by multicolor competition assays in HMECs in the presence or absence of nutlin-3a for approximately 3 PDs. Cells expressing either negative control luciferase (Luc) shRNA or mock infected serve as negative controls in HMECs expressing GFP (green fluorescent protein), and cells expressing shRNAs against either p21 or p53 serve as positive controls. Data is plotted as normalized percent of candidate shRNA in mix, i.e. ratio of GFP positive to GFP negative cell populations.

Supplemental Figure 3.

(A) Light microscope images of SA-β-Gal staining in BJ fibroblasts expressing the indicated shRNAs. **(B)** Multicolor competition assays in HCT116 cells in the presence or absence of nutlin-3a for approximately 3 PDs. Cells expressing either negative control luciferase (Luc) shRNA or mock infected serve as negative controls, and cells expressing shRNAs against either p21 or p53 serve as positive controls. Data is plotted as normalized percent of candidate shRNA in mix. **(C)** PDs in BJ fibroblasts expressing HPV E7 and the indicated shRNAs, with shRNAs

against p53 and $p21^{CIP1}$ as positive controls. **(D)** Western blots in E7 BJs for the indicated proteins expressing the indicated shRNAs. **(E)** RT-qPCR for p53 expression in mid-passage BJ fibroblasts expressing the indicated shRNAs. **(F)** Western blot analysis of mid-passage BJ or late-passage E7 BJ cells expressing the indicated shRNAs. **(G)** RT-qPCR for GATA4 expression in BJ fibroblasts expressing USP28 or an empty vector. **(H)** Western blot analysis of BJ cells expressing a Dox-inducible viral vector (Tet-ON) expressing USP28 and infected with a viral vector expressing the indicated shRNAs. Cells were treated with Dox for 7 days.

(I) Light microscopy images of SA-β-Gal staining in mid-passage BJ fibroblasts expressing either empty pBABE vector, WT USP28 or mutant USP28C171A. **(J)** PDs in mid-passage E7 BJ fibroblasts expressing the indicated pBABE retroviral constructs, including empty vector, WT USP28, and $USP28^{C171A}$. **(K)** Western blot three days post-infection with empty vector or WT USP28 with the indicated antibodies in mid-passage E7 BJ fibroblasts expressing the indicated constructs. **(L)** SA-β-Gal staining of cells used in Figure 3C. Data are mean ± SEM; Statistical significance was calculated by two-tailed Student's t test. Data are representative of three independent experiments.

Supplemental Figure 4.

(A) SA-β-Gal staining on day 7 of Dox treatment of BJ cells constitutively expressing the indicated ORFs or shRNAs and infected with a Dox-inducible viral vector (Tet-ON) expressing either wild type USP28 (WT) or $USP28^{C171A}$ mutant. Data are mean ± SEM; Statistical significance was calculated by one-way ANOVA.

(B) Heat map of copy-number analysis of USP28 in normal tissue and tumor samples, showing the location of the USP28 locus. **(C)** Percentages of USP28 deletions occurring in the indicated collections of cancer cell lines and tumor samples. **(D)** Tumor type-specific distribution of USP28 and SMAD2 in human cancers from a collection of 8200 tumors, also showing type of mutation.

Supplemental Table S1.

Log2 ratios for shRNAs which increased cell lifespan in E6 BJ fibroblasts in the pilot screen.

Supplemental Table S2.

Log2 ratios for shRNAs which increased cell lifespan in E6 BJ fibroblasts in the primary genome screen.

Supplemental Table S3.
Log2 ratios for shRNAs which increased cell lifespan in E7 BJ fibroblasts in the pilot screen.

Supplemental Table S4.
Log2 ratios for shRNAs which increased cell lifespan in E7 BJ fibroblasts in the primary genome screen.

Supplemental Table S5.
Log2 difference ratios for shRNAs which exhibited nutlin resistance in HCT116 colon cancer cells in the pilot screen.

Supplemental Table S6.
Log2 difference ratios for shRNAs which exhibited nutlin resistance in human mammary epithelial cells (HMECs) in the pilot screen.

Supplemental Table S7.
Log2 difference ratios for shRNAs which exhibited nutlin resistance in human mammary epithelial cells (HMECs) in the primary genome screen.

Supplemental Table S8.
Gene symbols for genes targeted by shRNAs that scored positively in the nutlin-resistance pilot screens in both HMEC and HCT116 cell lines.

Supplemental Table S9. Genes which scored positively in nutlin-resistance multicolor competition validation assays in HMECs. shRNAs that met a candidate criteria of a nutlin log2 difference of 1 or higher in three different experiments were considered positive, validated shRNAs.

Supplemental Table S10. Genes commonly identified in the nutlin-resistance screens and senescence-bypass screens. Genes that met candidate criteria in either focused or genome scale libraries for nutlin-resistance in HMECs and senescence-resistance in E7 BJ fibroblasts were included.

Supplemental Table S11.

Annotation of the senescence validation library showing the included genes, how many shRNAs targeted each gene, and the corresponding shRNA sequences.

Supplemental Table S12.

Candidate shRNAs which increased cell lifespan in E6 BJ fibroblasts in the validation screen.

Supplemental Table S13.

Candidate shRNAs which increased cell lifespan in E7 BJ fibroblasts in the validation screen.

Supplemental Table S14.

Candidate shRNAs which increased cell lifespan in naive BJ fibroblasts in the validation screen.

Mazzucco et al. Supplemental Figure 1

A

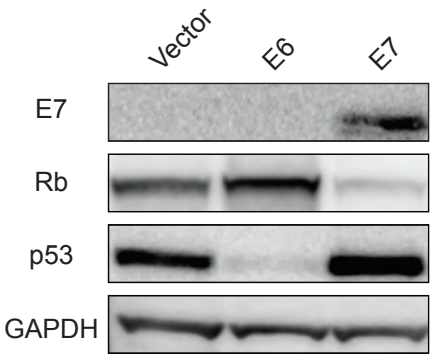

B

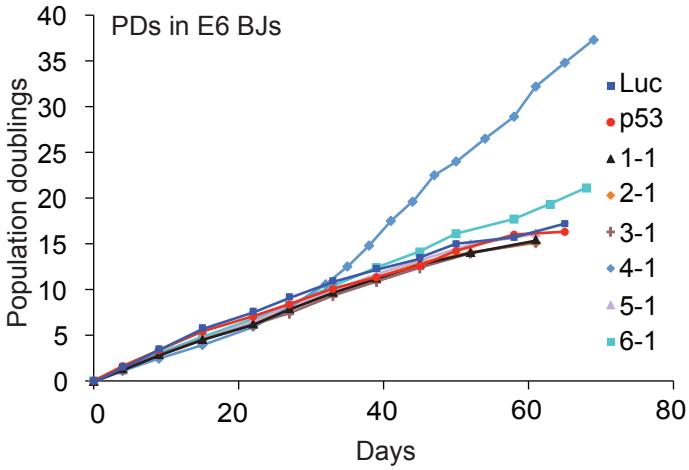

C

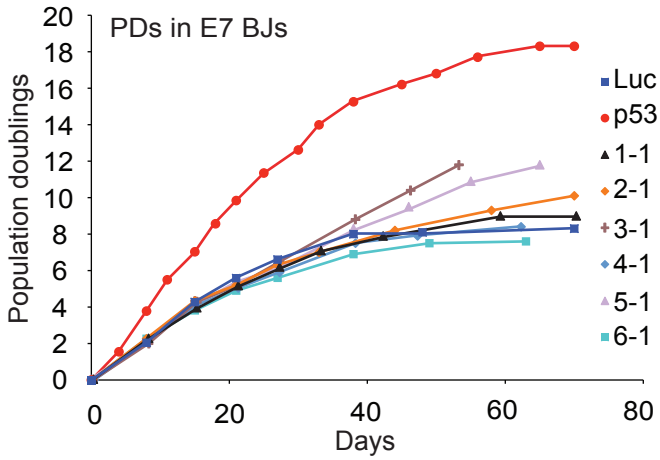

Mazzucco et al. Supplemental Figure 2

A

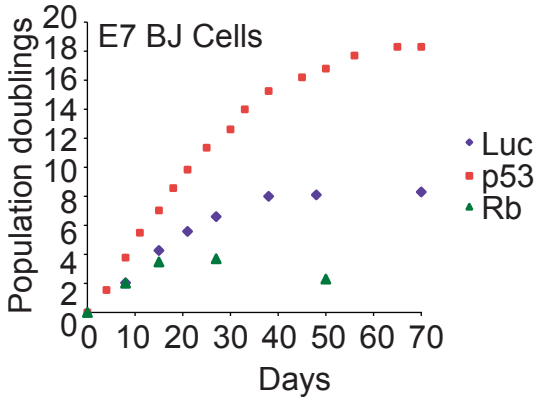

B

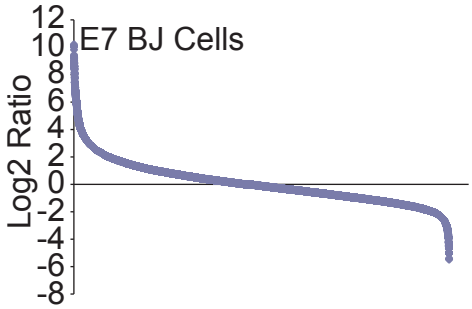

C

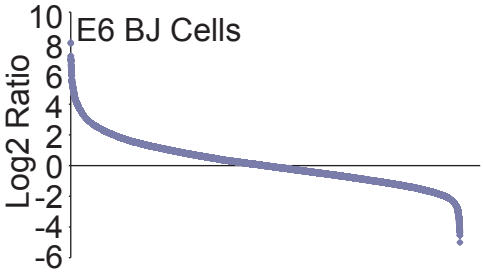

D

E6 BJ screens known proliferation regulators
CDKN2A (p16)
RB1
CDKN1C (p57)
CDKN2C (p18)
PTEN
CDKN1A (p21)

E

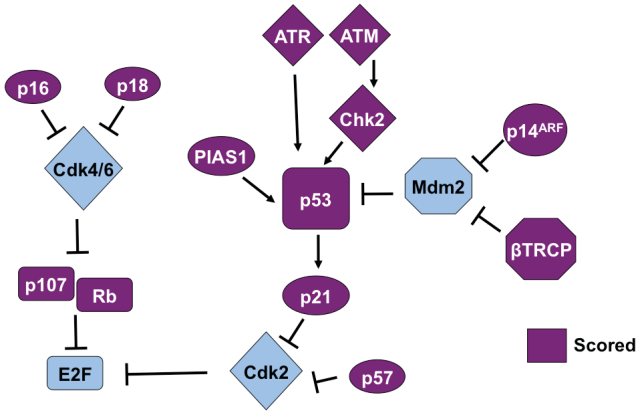

F

E7 BJ screens known p53 pathway cell cycle components
TP53 (p53)
CDKN1A (p21)
ATM
CDKN2A (p16)
BTRC (βTRCP)
USP28
ATR
CHEK2
PIAS1
BRD7
PBRM1 (BAF180)
HMGB1
TGFβR1
TGFβ1

G

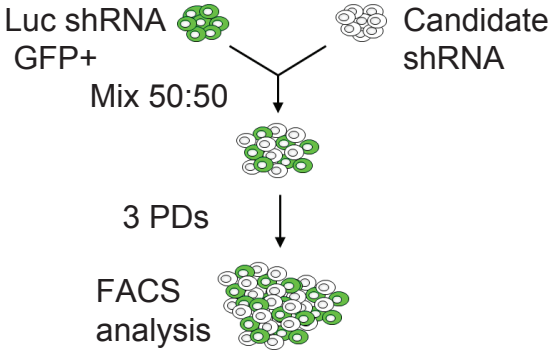

H

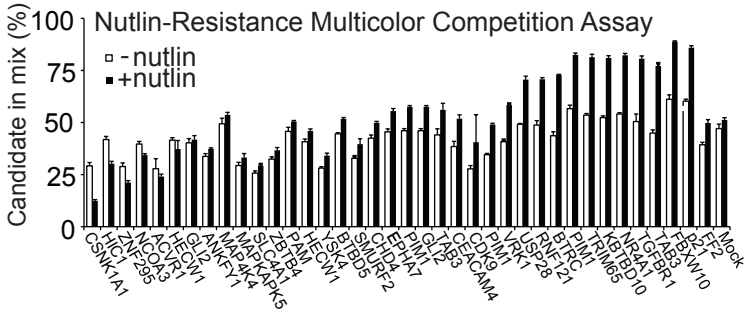

Mazzucco et al. Supplemental Figure 3

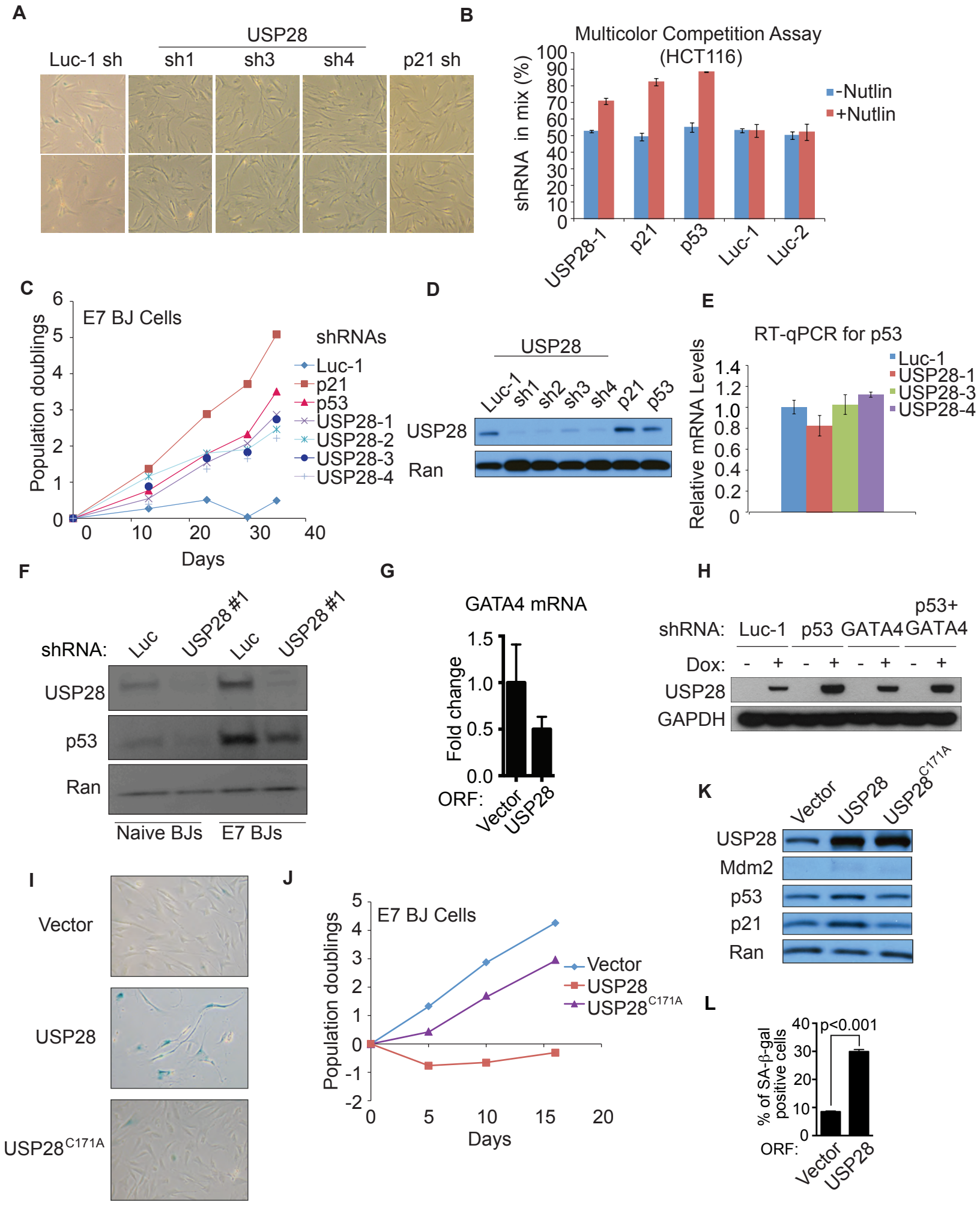

Mazzucco et al. Supplemental Figure 2

A

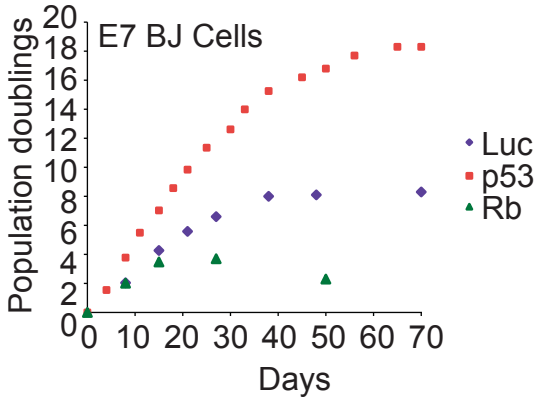

B

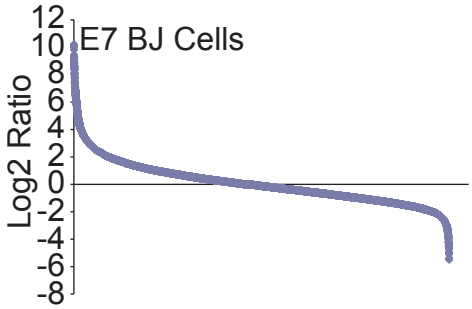

C

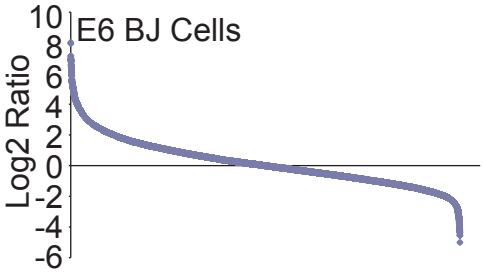

D

E6 BJ screens known proliferation regulators
CDKN2A (p16)
RB1
CDKN1C (p57)
CDKN2C (p18)
PTEN
CDKN1A (p21)

E

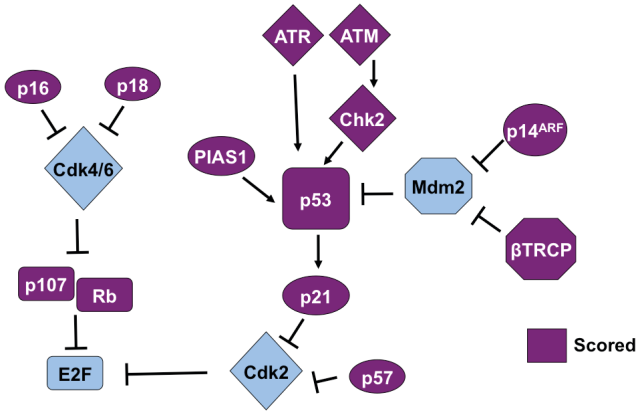

F

E7 BJ screens known p53 pathway cell cycle components
TP53 (p53)
CDKN1A (p21)
ATM
CDKN2A (p16)
BTRC (βTRCP)
USP28
ATR
CHEK2
PIAS1
BRD7
PBRM1 (BAF180)
HMGB1
TGFβR1
TGFβ1

G

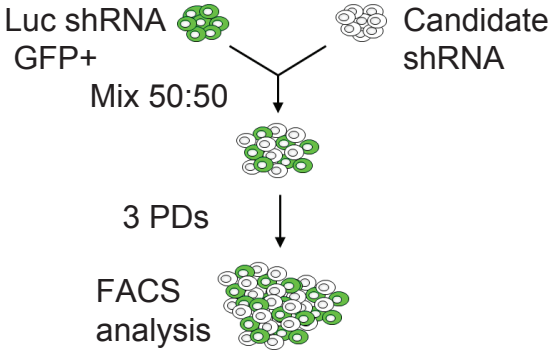

H